Available online at www.sciencedirect.com
SCIENCE DIRECT
Applied Catalysis A: General 291 (2005) 13–20
APPLIED CATALYSIS A: GENERAL
www.elsevier.com/locate/apcata

CO oxidation on gold nanoparticles: Theoretical studies

Ioannis N. Remediakis [a], Nuria Lopez [b], Jens K. Nørskov [a,*]

[a] Center for Atomic-scale Materials Physics, Department of Physics, Technical University of Denmark, 2800 Lyngby, Denmark
[b] Department Quimica Fisica, Universitat de Barcelona, C/Marti i Franques 1, 08028 Barcelona, Spain

Received 11 November 2004; received in revised form 3 January 2005; accepted 3 January 2005
Available online 27 June 2005

Abstract

We present a summary of our theoretical results regarding CO oxidation on both oxide-supported and isolated gold nanoparticles. Using Density Functional Theory we have studied the adsorption of molecules and the oxidation reaction of CO on gold clusters. Low-coordinated sites on the gold nanoparticles can adsorb small inorganic molecules such as O_2 and CO, and the presence of these sites is the key factor for the catalytic properties of supported gold nanoclusters. Other contributions, induced by the presence of the support, can provide parallel channels for the reaction and modulate the final efficiency of Au-based catalysts. Finally, our theoretical simulations allow us to discuss the selectivity of supported Au nanoparticles.

Keywords: Density functional calculations; Gold; Oxidation; Titanium oxide; Nanoparticle

1. Introduction

Gold is known to be the noblest of all the metals [1], although, since the work performed in the group of Haruta et al. [2] it is well-established that the nobility of gold disappears for nanometric-size particles. In fact, those particles are active for CO oxidation at room temperatures; partial oxidation processes, i.e. propylene oxidation; NO reduction by CO; the water gas shift (WGS) reaction and selective elimination of CO from H_2 containing gases. [3]

For CO oxidation, the turn-over frequency (TOF) depends mainly on the size of the gold nanoparticle, the most reactive ones being in the 2–4 nm range. [4] The TOF also depends on the preparation method and the support. [3] Nowadays, active Au nanoparticles are prepared as dispersions on reducible (TiO_2, NiO or Fe_2O_3 [2]) or irreducible (Al_2O_3 and $MgAl_2O_4$ [5–7]) oxides, or, more recently, on activated carbon fibers [8] or even without any support, in the form of gold nanotubes [9]. A multitude of factors have been proposed in order to explain the enhanced catalytic activity of gold nanoparticles, and the active site for CO oxidation has been suggested to be either on the metal or at specific ensemble sites at the interface between the metal and the support. The proposed mechanisms can be classified in terms of the degree of dependence on the support as follows:

- *Gold-only mechanisms*: This category includes mechanisms where low-coordinated Au atoms in gold nanoparticles act as the active sites, and those that benefit from the effect of odd–even transitions and quantum size effects [4]. Undercoordinated gold sites can act as centers for the adsorption of molecules [10–15], therefore the roughness of the surface has been proposed as an indicator of its activity [16]. Due to the finite size of the supported nanoparticles, undercoordinated centers are more abundant in a nanoparticle compared to a single-crystal [10]. On the other hand, odd–even transitions have been reported to have an important role in the reactivity of small gas-phase gold clusters and gold subnanometer structures [17,18].
- *Support induced mechanisms*: In these cases, the support could either charge the gold nanoparticle [17] or induce strain in the Au structures that can affect the reactivity of the supported metal [10,19]. EXAFS experiments performed on real catalysts [20] give no indication of

* Corresponding author.

0926-860X/$ – see front matter © 2005 Elsevier B.V. All rights reserved.
doi:10.1016/j.apcata.2005.01.052

significant changes in the gold–gold distances. With respect to charging, it has been found that it can be relevant in the case of isolated metal atoms or subnanometer structures [17,21]. For larger metallic structures, however, charge is screened quite efficiently and its effect decays exponentially with the distance from the charged center [22].

- *Support driven and support-assisted mechanisms*: This group of mechanisms include situations where the support provides activated oxygen [23], or stabilizes reactants and intermediates [15,24]. The role of the support as O_2 provider has been ruled out as the main contribution in gold-based catalysts, as the reaction can also take place on reducible carriers, like $MgAl_2O_4$ [7]. However, reducible supports can trap incoming O_2 molecules and in that way enhance the performance of some catalysts by improving mass transport of the reactants to the reaction site [25]. In addition, the support can stabilize some species along the reaction path either by polarization effects [26] or by direct bonding, e.g. of O_2 to one Au atom and one atom from the support [15,24,27]. In the latter case, if the reaction ensemble is placed at the interface, the mechanism is usually referred to as *metal/oxide boundary* mechanism.

However, the above classification is rather schematic, since in a given system more than one of the above mechanisms may be taking place. For instance, the substrate redox properties affect the dispersion and the shape of the supported nanoparticles [20,28] but they also control the charge transfer at the interface and the ability of the support to trap the reactants. This is the reason why it is a very challenging task to distinguish experimentally between the aforementioned mechanisms, and find the dominant one in each case. On the other hand, first principles Density Functional Theory (DFT) calculations can provide a clearer insight into the CO oxidation on supported gold nanoparticles. The procedure we follow is to increase the complexity of the model employed by obtaining the contributions from the finite size effect of the gold particle and the effect of the support in a subsequent step. This procedure allows the identification of the different aspects involved in the catalyst by gold and provides the quantitative contribution of the different factors linking them to the structure and composition of the system [11,27]. The system chosen is Au/TiO_2 since it is the most deeply investigated Au-based catalyst, and several aspects of its activity and its structure, up to the atomistic level, have been investigated [4,28]. CO oxidation is taken as the model reaction for the same reasons.

2. Technical details

The calculations were carried out using Density Functional Theory. The DACAPO package was employed [29]. The ionic cores and their interaction with valence electrons were described by ultra soft pseudopotentials [30]. Exchange and correlation effects were taken into account via the Generalized Gradient Approximation (GGA) and the revised Perdew–Burke–Ernzerhof (RPBE) functional [31]. The wave function was expanded in a plane-wave basis with a kinetic energy cutoff of 25 Ry. The valence electron density is obtained by self-consistent iterative diagonalization of the Hamiltonian [32], with Pulay mixing of the output and input densities [33]. Occupation of the one-electron states was calculated using a temperature of $k_BT = 0.2$ eV; all energies have been extrapolated to $T = 0$ K. The ionic degrees of freedom were relaxed using a conjugate-gradient minimization, until the root of the mean squared force component was smaller than 0.05 and 0.2 eV/Å for the rigid and the flexible clusters, respectively. For the large systems containing the flexible clusters a further relaxation of selected structures results in insignificant changes in the calculated energies. When the transition states have been located through constrained minimization, the forces on the atoms are smaller than 0.3 eV/Å leading to energies converged up to 0.05 eV. The rigid unsupported clusters were built with a fcc structure keeping the (1 1 1) and (1 0 0) facets observed in the supported particles. They were calculated in a 15 Å cubic box with a single k-point. The TiO_2(1 1 0) substrate was modeled by a two-layered slab and a (4×2) surface unit cell. Subsequent slabs are separated by about 15 Å of vacuum; even when CO is adsorbed on the gold cluster, the minimum distance between slabs is more than 6.5 Å. Although the energies of vacancy formation and O_2 adsorption are strongly dependent on the number of TiO_2 layers [34], the huge size of the calculation prevented us to use thicker supercells. However, the final structure employed contains the structural and chemical complexity of dispersed supported nanoparticles and allows the identification of the relevant terms in the reaction process. The computational effort required for the detailed theoretical study of even a simple chemical process as CO oxidation is enormous.

3. CO oxidation

To unravel all possible contributions coming from the presence of the support in a gold catalyst, we compare the reactivity of a gold nanoparticle in different environments. Our starting structure is a rigid model, Au_{10} particle, that mimics the shape of a flat nanoparticle and shows the (1 1 1) and (1 0 0) characteristic faces of larger particles. In a second step, the same Au_{10} particle has been supported on an oxygen deficient rutile TiO_2(1 1 0), and all gold atoms and the first rutile layer have been relaxed without constraints. To identify the electronic effect of the support we have considered the same structure that the gold cluster would have if supported, but without the support. This procedure deconvolutes the electronic and the geometric constraints induced by the support. In the two latter cases, contributions

from the metal cluster fluxional character are, at least partially, included.

3.1. Isolated rigid Au_{10} nanoparticle

The calculations for a rigid Au cluster illustrate the role that low-coordinated atoms play in the enhanced reactivity of gold. The starting geometry of the Au_{10} nanoparticle shows a basal plane of (1 1 1) character and lateral faces with (1 1 1) and (1 0 0) patterns. The Au coordination number is 5 for the gold atoms in the top layer and 4 for the periphery metal atoms on the basal layer. During relaxation of the atomic positions, the symmetry of the cluster as well as the z-coordinates of the basal Au atoms are kept fixed. After relaxation, we observe a small reduction in the Au–Au distance of the order of 0.08 Å with respect to bulk Au–Au distance, in agreement with the EXAFS results on real catalysts [20].

For the unsupported rigid particle, CO and O_2 adsorption and CO oxidation were analyzed; the reaction path is shown in Fig. 1 [11]. The adsorption of CO on the particle is rather strong: CO adsorption energy is −0.6 eV, much lower than that for a step-edge site on Au(2 1 1), which is approximately −0.25 eV [20]. This structure can further adsorb an oxygen molecule in a μ_2 configuration, where the two O atoms are bonded to a Au center each, with an adsorption energy of −0.3 eV. The adsorption of O_2 on the gold nanoparticle can only proceed at the very low-coordinated sites on highly defective Au surfaces. This correlates with the upward shift (about 0.75 eV) of the d-band center from the Au(1 1 1) surface to the Au atoms in the periphery of the Au_{10} cluster. It has been demonstrated that for a given metal atom in different environments the closer the d-band center is to the Fermi level the more prone towards adsorption the site is [1].

After adsorption, the reaction can proceed via two different pathways similar to those reported for Pt [35]. The first one is the direct CO–O_2 coupling that shows an energy barrier of 0.40 eV. The final O atom that remains on the particle can be eliminated by a second CO molecule at a much lower cost; the energy barrier is only 0.16 eV. The indirect path takes place through the dissociation of the O_2 molecule. For the rigid Au_{10} particle, O_2 can easily dissociate to form two adsorbed O atoms, at the corner site. The energy barrier for this process is dissociation pathway is very sensitive to the geometry. For instance, dissociation of O_2 from the μ_2 state to two adsorbed O atoms, one of which is adsorbed on the basal Au plane while the other is adsorbed on the top plane, shows a much larger barrier, close to 1 eV. Again, the adsorbed isolated O atoms can be easily removed by the incoming CO molecules as in the second step for the direct mechanism.

3.2. Supported gold nanoparticle

In a second step, we deposited the Au_{10} cluster on the defective rutile TiO_2(1 1 0) [27]. At room temperature and pressure, gold nanoparticles do not bind to the perfect rutile TiO_2(1 1 0) [36]. However, under the same conditions, reducible oxides like rutile contain a certain amount of oxygen vacancies that act as anchoring points [28]. For a normal sample preparation used in STM experiments, about 7–10% of the surface O atoms are missing [37]. Low temperature STM experiments have shown that the most frequently observed gold nanostructures, containing up to 30 gold atoms, present a ratio of about three Au atoms per oxygen vacancy [28]. To reproduce the effect in our model, the Au_{10} cluster is set up to bond through three missing O atoms from the bridging oxygen rows. The relaxed geometry is shown in Fig. 2. After relaxation of the supported Au_{10} cluster the Au–Au distances are similar to the original, but the average coordination number of the Au atoms has increased and thus the surface energy of the system has been

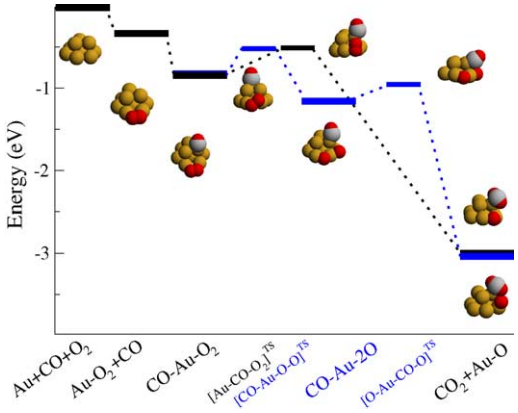

Fig. 1. Reaction path for CO oxidation on the isolated rigid Au_{10} cluster. Au, C and O atoms are represented by yellow, gray and red spheres, respectively. The blue line represents the indirect path while the black line corresponds to the direct path. (For interpretation of the references to color in this figure legend, the reader is referred to the web version of this article.)

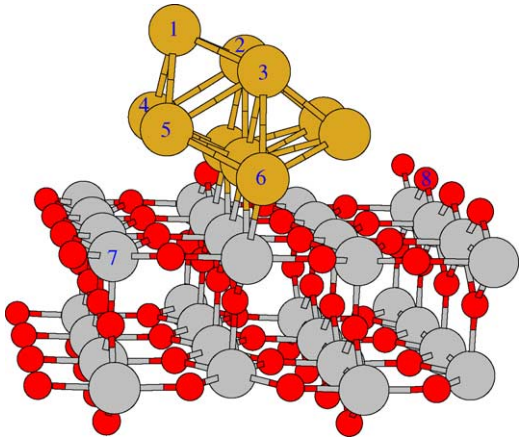

Fig. 2. Relaxed geometry for an Au_{10} cluster supported on reduced TiO_2(1 1 0). Au, Ti and O atoms are represented by yellow, gray and red spheres, respectively. Structure is periodic in both lateral dimensions. (For interpretation of the references to color in this figure legend, the reader is referred to the web version of this article.)

reduced. Only one Au reduces its coordination number when compared to the rigid model (atom number 1 in Fig. 2).

For this supported cluster, we only consider adsorption of CO, O_2, O and CO_2 and the direct CO + O_2 oxidation path. To reduce the size of the calculations only some characteristic geometries, resembling of those found for the rigid cluster, were explored, and only Au and adsorbate atoms were relaxed. The adsorption energies for all considered configurations are shown in Table 1. CO binds with the same adsorption energy atop the highest Au atom and between the two highest ones. The adsorption energy is −0.95 eV, higher than the energy that reported for the rigid cluster −0.60 eV, due to the reduced coordination of the Au atom in the supported cluster, 4 versus 5 in the previous case. Recently, Meier and Goodman [38] have reported singleton CO binding energy for CO on TiO_2 supported Au bilayer clusters of 0.8 and 0.5 eV for unsupported ones. Within the error bar of the experiments, these values are essentially the same as the computed ones.

On the other hand, O_2 has a preference for binding in the contact area between the Au cluster and the Ti(5c) on the surface. One of the O atoms of the O_2 molecule binds to a periphery Au atom, while the second bonds to a Ti atom of the support. The binding energy to this site is −1.59 eV relative to gas-phase CO and O_2. This value is only marginally affected, by 0.05 eV or less, by changes in the redox characteristics of the neighboring sites, i.e. by removing a bridging O from TiO_2 or adding a spectator O_2 molecule far away from the adsorbates. This configuration is the initial point for a *support-assisted or metal/oxide boundary* mechanism, where the substrate stabilizes the reactants. Other low-coordinated gold atoms can provide a site for O_2 binding without any direct interaction to the oxide. The reduced size of the cluster employed makes the location of such a center difficult but the bridge site between Au atoms 5 and 8, with the constraint on the z position of the O atom closer to the support, can be representative of such configurations. This structure has an energy of −1.15 eV relative to gas-phase CO and O_2, similar to the −0.9 eV stand-alone Au_{10} particle and constitutes the starting point for a *gold-only* mechanism.

Table 1
Adsorption energies for configurations of the considered species on rutile-supported Au_{10}

Adsorbate (adsorption sites)	Energy (eV)
CO (atop, 1)	−0.95
CO (bridge, 1,2)	−0.95
CO (atop, 1) + O_2 (bridge, 4,5)	−1.59
CO (atop, 1) + O_2 (bridge, 5,6, constrained)	−1.15
CO (atop, 1) + O_2 (bridge, 5,6)	−1.32
CO (atop, 1) + O_2 (bridge, 3,5)	−0.57
CO (hollow, 1,2,3) + O_2 (bridge, 1,4)	−0.10
TS: CO (atop, 1) + O_2 (atop, 5)	−0.79
TS: CO (atop, 5) + O_2 (atop, 5 and Ti)	−1.19
CO_2 (atop, 1) + O (bridge, 1,5)	−4.06
CO (bridge, 2,3) + O (bridge, 1,5)	−0.63
CO_2 (atop, 1)	−3.66

The numbers next to each molecule refer to the labels of Au atoms in Fig. 2. Energies are relative to gas-phase CO and O_2. The configurations whose energies are used in Fig. 3 are typed in bold. The adsorption energy for CO_2 is −0.48 eV relative to the gas phase.

The energy barrier for direct oxidation, CO + O_2 → CO_2 + O, on the rutile-supported Au cluster through the *gold-only* mechanism was estimated by considering CO and O_2 in a configuration similar to that found for the isolated rigid Au_{10} particle. The C–O bond length was fixed at the transition state value, 2.8 Å, while all other degrees of freedom of the adsorbate and the gold atoms were relaxed. The so calculated energy barrier is 0.36 eV with respect to adsorbed CO and O_2. For the *metal/oxide boundary* mechanism the CO + O_2 coupling path has been located by modifying the C–O distance until we the maximum energy is found, while the O_2 is placed at the interface. The calculation was performed in both ways, once increasing the C–O bond length, going from CO_2 to CO and the second time decreasing the distance, thus going from CO + O to CO_2. In such a way the actual energy barrier should be close to the value we obtain for the highest energy point which is similar in both directions. At the transition state, CO is bonded to the top gold atom in Fig. 2. The O–O distance is 1.4 Å and the C–O distance is 1.8 Å. The second O atom that does not participate directly to the oxidation, sits on top of a ''bare'' Ti atom, with an O–Ti distance of 2.3 Å. This path has an energy barrier (from adsorbed CO and O_2) of 0.40 eV similar to the reported in for the gold-only mechanism. For both transition state structures the forces on the ions were small, indicating that the system is indeed in a saddle point.

The two different final states, CO_2 + O, corresponding to the *metal/oxide boundary* mechanism and to the *gold-only* mechanism were also identified. In the first case, the O_{ads} is sitting at the metal-oxide boundary, and is placed at −3.88 eV, while in the second case O_{ads} it is placed at the particle, with an energy of −4.06 eV. In any case, the final state CO_2 + O has a lower energy than for the isolated rigid Au_{10}, which was −3.20 eV. In fact, for gas-phase Au clusters the adsorption of O atoms largely distorts the cluster structure [14]. This phenomenon is not observed in the rigid model due to the geometry constraints imposed. O-induced distortions might contribute to the rapid deactivation observed for the activity of supported gold clusters. Moreover, since adsorbate induced reforming is strongly related to the average coordination number of all the atoms in the metallic nanoparticle, reformation will preferentially affect very small particles. This could explain the low activity of clusters below 1 nm [4].

3.3. Unsupported flexible Au_{10} cluster

In order to estimate the oxide-induced contributions to the *gold-only* mechanism, the energies of the initial, final and transition states for an unsupported flexible Au_{10} cluster were calculated. The presence of the oxide was simulated by

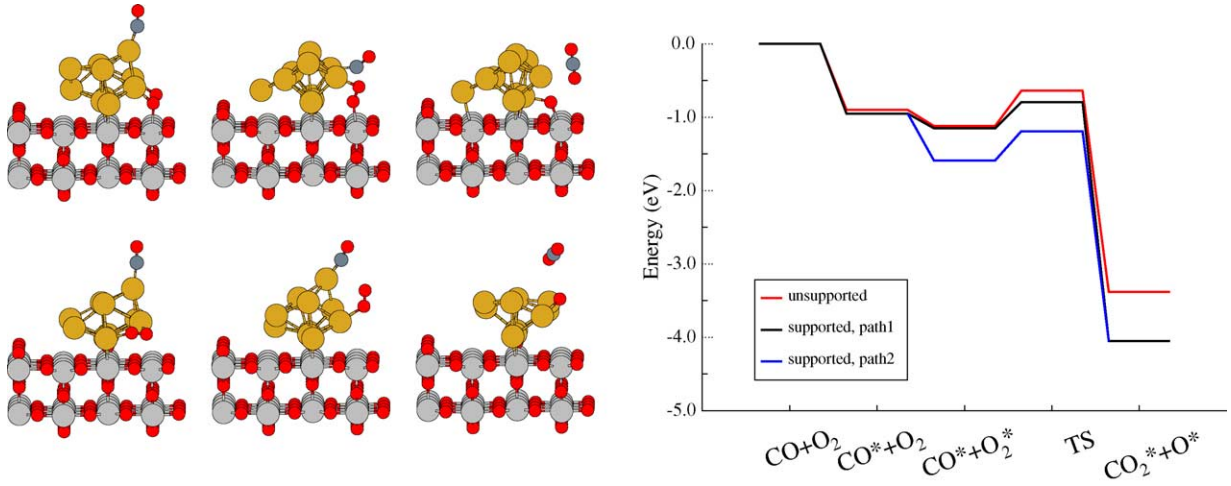

Fig. 3. Compared geometries (left) and energy profiles (right) for the CO oxidation on a Au_{10} cluster. Upper panel, blue line: Au_{10} supported on TiO_2(1 1 0), CO oxidation takes place on the Au/TiO_2 interface. Lower panel, black line: Au_{10} supported on TiO_2(1 1 0), CO oxidation takes place solely on Au particle. Red line: Unsupported cluster with the bottom three atoms kept fixed at the positions they would have if the oxide was present. (For interpretation of the references to color in this figure legend, the reader is referred to the web version of this article.)

fixing the bottom three atoms (numbered 8–10 in Fig. 2) at the positions they had in the initial state of the supported cluster. As a consequence, geometric contributions are only partially taken into account while the electronic effects coming from the support are completely removed. All other Au atoms and adsorbates are fully relaxed, except for the transition state, where the C–O bond was kept fixed. The comparison between the energetics of the unsupported and the supported cluster is shown in Fig. 3. The adsorption energy for CO on the unsupported gold cluster is −0.90 eV, similar to that of the supported cluster (−0.95 eV). This also holds for the co-adsorbed CO and O_2 state: −1.12 eV for the unsupported cluster (−1.15 eV for the supported). The transition state energy, however, is 0.15 eV higher for the unsupported cluster, yielding an energy barrier of 0.48 eV. The final state CO_2 and O, has an energy closer to that to the rigid cluster, −3.20 eV, due to the geometric constraints imposed.

3.4. Discussion

For the above gold-based systems, all the CO oxidation paths reported show similar activation energies 0.36–0.40 eV, for the rate limiting step. This is similar to the value measured by Haruta et al. [2], close to the range 0.15–0.25 eV given for STM characterized catalysts [39] and within the broad range of 0.16–0.60 eV reported by other authors [40,41]. As a consequence, all the aforementioned Au nanoparticles appear to be better catalysts for CO oxidation than any single-crystal transition metal catalyst. For example, on Pt(1 1 1), O_2 adsorbs in a precursor state and dissociates through a small barrier 0.46 eV [35]. The adsorbed O atoms are, however, strongly bond to Pt(1 1 1) and thus the next step, CO–O coupling, shows a large energy barrier (0.75 eV) due to the large stabilization of the reactants. In the present case, the noble nature of gold prevents a strong adsorption of O atoms and molecules even when very low-coordinated atoms exists. This mild bonding character is at the basis of gold-based catalysts in oxidation processes at low temperatures. Moreover, a broad range of binding energies, about 1 eV, going from slightly repulsive to weakly attractive can be attainable by controlling the coordination number of Au.

Gold-based catalysts may also benefit from the presence of the support. First, the support favors and stabilizes metal dispersion and a given shape. As shown by Mavrikakis et al. [10], a high dispersion increases the relative number of low-coordinated sites and therefore the number of reaction sites for *gold-only* mechanisms. The electronic contributions due to the presence of the rutile support to the *gold-only* mechanism can be investigated from the density difference between the supported particle and the free particle, shown in Fig. 4. In this figure, we plot the difference between the charge density of the Au_{10}/reduced TiO_2(1 1 0) system minus the sum of the charge densities of Au_{10} (at the same geometry) and reduced TiO_2(1 1 0). Charge is accumulated between Au and Ti atoms, and the electrons trapped in the O-deficient substrate are employed to furnish the bonds at the interface. The Au atoms of the second layer, however, are not affected by the presence of the support. In addition, the added charge resides at the Au-substrate interface. This is mirrored in the positions of the d-band centers for Au atoms that are changed only marginally between the free and the supported cluster. These observations do not lend any support to the possibility of a support driven mechanism based on metal charging. This explains why only small differences are found for supported and unsupported Au_{10} in the previous sections and indicates that both dispersion

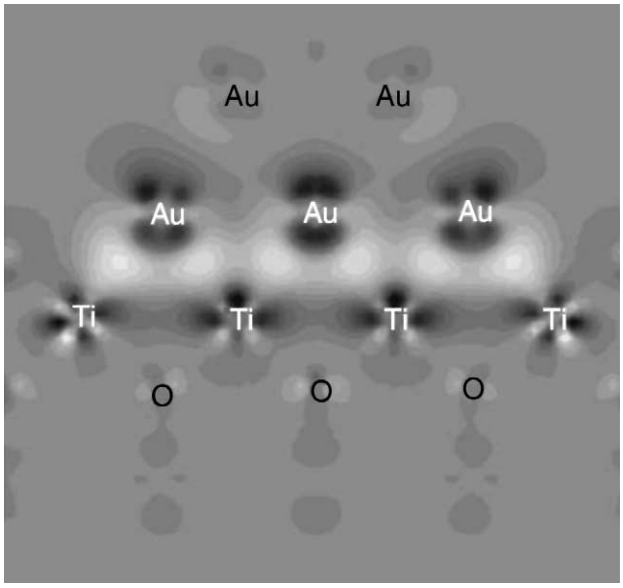

Fig. 4. Contour plot of the density difference along the (0 0 1) direction between the Au_{10}/reduced TiO_2 minus the sum of charge densities of Au_{10} and the reduced TiO_2(1 1 0). Background gray color denotes zero difference. Lighter (darker) color denotes higher (lower) local electron density.

(size) and shape are the main contributions from the support in *gold-only* mechanisms.

Moreover, the presence of the support can provide additional channels for the reaction to occur, as happens for the Au/TiO_2 system. In that case, the metal/support interface presents special complex ensembles that contain both undercoordinated Au and support-atoms act as reaction sites in *metal/oxide boundary* mechanisms. These complex ensembles depend on the support structure and properties and therefore should be analyzed for each substrate.

In addition, the presence of a *gold-only* reaction pathway that is common for all supports explains why very different supports have been successfully employed; since there is always an open channel based only on the chemical activity of low-coordinated Au atoms. The simultaneous presence of a second mechanism taking place at the *metal/oxide boundary*, that enhances the activity of the system and is substrate dependent, explains the different activity observed for different gold-based catalyst. In both reaction paths a high concentration of low-coordinated gold atoms is required to bind the reactants. As a consequence, the gold particle size, a measure of the number of low-coordinated Au atoms, is found to be the main parameter governing the reactivity of gold-based catalysts. [13]

3.5. CO versus H_2 oxidation, selectivity

One of the potential uses for Au-based catalysts is in the cleaning of the H_2 gas feed to fuel cells. In a Proton Exchange Membrane (PEM) fuel cell, hydrogen produced by hydrocarbon and alcohol reforming is supplied to the anode where it oxidizes, thus generating electrons that flow through the external circuit and protons that react with O_2 at the cathode. The anode catalyst is severely poisoned by CO present in the H_2 gas feed. CO concentrations as small as 100 ppm can completely block the active sites on Pt or modified Pt surfaces typically employed as anode electrodes. To avoid this problem, it has been proposed to selectively oxidize CO from the H_2 feed by means of Au-based catalysts [2,42]. The so-called preferential oxidation of CO, PROX, reaction has been addressed theoretically by Mavrikakis et al. They studied the adsorption of several intermediates in the oxidation reactions for Cu, Pt and Au on the (1 1 1) surfaces, where water formation shows larger energy barriers than CO oxidation [43]. Moreover, in kinetic experiments it has been proposed that the H_2 activation/dissociation can be the rate determining step [42]. For Au(1 1 1) surfaces the reaction is endothermic by 0.5 eV and has a barrier of 1.2 eV (within the PW91 approach) [1], but for very small gas-phase, Au_n (n = 2 and 3) clusters, dissociation barriers of 0.55 and −0.12 eV, with respect to gas-phase reactants, have been reported [44]. Negative barriers arise from the presence of a molecularly adsorbed H_2 species previous to dissociation.

To oxidize either hydrogen or CO, the molecules should be adsorbed before they react with O_2. CO adsorption on Au_{10} is a non-activated process while a barrier is found for the dissociative adsorption of H_2 on several metal surfaces including Au(1 1 1). We have investigated several paths for the adsorption of H_2 to the rigid Au_{10} cluster. The final states considered are such that H atoms are adsorbed in between two Au atoms either on the top layer or at the basal plane. For a site on the rigid Au_{10} cluster with coordination number of 5 (top layer), the dissociated state is still endothermic for H_2, +0.47 eV, and hindered by a sizeable barrier close to 1 eV, while CO adsorption at the same site is exothermic by −0.6 eV. In the case of a competitive activated (H_2) and non-activated (CO) adsorption process the ratio of initial adsorption rates on the catalyst surface can be written as follows [45]:

$$\frac{r_{CO}}{r_{H_2}} \approx \frac{p_{CO}}{p_{H_2}\exp(-\Delta E/RT)} \quad (1)$$

where r_{CO} and r_{H_2} are the initial adsorption rates, p the pressures of CO and H_2 and ΔE are the barrier for H_2 adsorption. With the previous values for the adsorption of CO and H_2 barrier we find that at room temperature and with a H_2 feed of 1 atm containing 100 ppm of CO, the initial adsorption rate is still several orders of magnitude larger for CO than for H_2. Therefore, the selective CO elimination from H_2 feeds can be understood, at least partially, from the fact that a larger fraction of sites would be covered by CO preventing H_2 oxidation.

Finally, we want to point out that the barriers for H_2 dissociation were found to be dependent on the gold structure. For example, Morikawa [47] has found a much lower barriers for H_2 dissociation on gold chains. A large

contribution from reforming in very small Au clusters is also expected from the results of Varganov et al. [44]. This large dependence on the coordination number in the very small cluster regime might explain the selectivity observed for other reactions. For instance, propylene epoxidation in the presence of O_2 and H_2 yields the oxidation product (for 2 nm Au nanoparticles) or the hydrogenated one (for particles smaller than 1 nm) [48].

4. Conclusions

Theoretical methods are capable of analyzing the possible contributions to the enhanced activity of gold. We have investigated several of these contributions by analyzing CO oxidation on a small (∼0.7 nm) gold cluster, standalone and supported on rutile TiO_2. According to the calculations, and in agreement with the experimental results, the presence of low-coordinated Au sites seems to be crucial for CO oxidation. Moreover, for supported gold catalysts two types of mechanisms have been identified. *Gold-only* mechanisms for which the reaction takes place only on the nanoparticle, in that case, the role of the support is that of changing the dispersion and shape of the cluster and the electronic contributions are found to be minor. Those mechanisms are therefore present in all the chemical preparations of Au-based catalyst irrespective of the support nature. A second branch of support-assisted *metal/oxide boundary* mechanisms may exist for which the reaction site is at the metal/oxide interface and the ensemble needed for O_2 adsorption requires both low-coordinated Au atoms in the gold particle and other centers on the oxide. In any case for the Au/TiO_2(1 1 0) system the calculated barriers of about 0.4 eV are in excellent agreement with the experimental results. For the preferential oxidation of CO in H_2 rich gases it is found that the barrier for H_2 dissociation is still too large, preventing a significant H_2 adsorption even in gases with a high H_2 partial pressure. All these aspects indicate that the particular chemistry of gold nanoparticles is still based on the noble character of gold, since the intermediates are not strongly bound to the surface and can easily react to form products. Finally, the challenging task in the development of new gold-based catalysts is the generation and stabilization of low-coordinated centers at the Au particles [46].

Acknowledgements

We acknowledge support from the Danish Center for Scientific Computing through grant no. HDW-1101-05. Discussions with B.S. Clausen, L.M. Molina, B. Hammer, F. Besenbacher, M. Mavrikakis, H. Metiu and D.W. Goodman are gratefully acknowledged. N.L. thanks MEC for financing her work through the RyC program and the Generalitat de Catalunya for a mobility grant BE2004.

References

[1] B. Hammer, J.K. Nørskov, Nature 376 (1995) 238.
[2] M. Haruta, S. Tsubota, T. Kobayashi, H. Kageyama, M.J. Genet, B. Delmon, J. Catal. 144 (1993) 175.
[3] M. Haruta, Catal. Today 36 (1997) 153.
[4] M. Valden, X. Lai, D.W. Goodman, Science 281 (1998) 1647.
[5] M. Okamura, S. Nakamura, S. Tsubota, T. Azuma, M. Haruta, Catal. Lett. 51 (1998) 53.
[6] S.-J. Lee, A. Gravriilidis, J. Catal. 206 (2002) 305.
[7] J.-D. Grunwaldt, H. Teunissen, Eur. Patent EP1209121, 2002.
[8] D.A. Bulushev, I. Yuranov, E.I. Suvorova, P.A. Buffat, L. Kiwi-Minsker, J. Catal. 224 (2004) 8.
[9] M.A. Sanchez-Castillo, C. Counto, W.B. Kim, J.A. Dumesic, Angew. Chem. Int. Ed. 43 (2004) 1140.
[10] M. Mavrikakis, P. Stoltze, J.K. Nørskov, Catal. Lett. 64 (2000) 101.
[11] N. Lopez, J.K. Nørskov, J. Am. Chem. Soc. 124 (2002) 11262.
[12] C. Lemire, R. Meyer, S. Shaikhutdinov, H.-J. Freund, Angew. Chem. Int. Ed. 43 (2004) 118.
[13] N. Lopez, T.V.W. Janssens, B. Clausen, Y. Xu, M. Mavrikakis, T. Bligaard, J.K. Nørskov, J. Catal. 223 (2004) 232.
[14] G. Mills, M.S. Gordon, H. Metiu, Chem. Phys. Lett. 359 (2002) 493.
[15] L.M. Molina, M.D. Rasmussen, B. Hammer, J. Chem. Phys. 120 (2004) 7673.
[16] G. Mills, M.S. Gordon, H. Metiu, J. Chem. Phys. 118 (2003) 4198.
[17] A. Sanchez, S. Abbet, U. Heiz, W.-D. Schneider, H. Häkkinen, R.N. Barnett, U. Landman, J. Phys. Chem. A 103 (1999) 9573.
[18] B. Yoon, H. Hakkinen, U. Landman, J. Phys. Chem. A 107 (2003) 4066.
[19] S. Giorgio, C. Henry, B. Pauwels, G.V. Tendeloo, Mat. Sci. Eng. A 297 (2001) 197.
[20] N. Lopez, J.K. Nørskov, T.V.W. Janssens, A. Carlsson, A. Puig-Molina, B.S. Clausen, J.-D. Grunwaldt, J. Catal. 225 (2004) 86.
[21] Q. Fu, H. Saltsburg, M. Flytzani-Stephanopoulos, Science 301 (2003) 935.
[22] L. Giordano, J. Goniakowski, G. Pacchioni, Phys. Rev. B 64 (2001) 075417.
[23] M. Schubert, S. Hackenberg, A. van Veen, M. Muhler, V. Plzak, R. Behm, J. Catal. 113 (2001) 197.
[24] Z.P. Liu, X. Gong, J. Kohanoff, C. Sanchez, P. Hu, Phys. Rev. Lett. 91 (2003) 266102.
[25] E. Walhström, E.K. Vestergaard, R. Schaub, A. Rønnau, M. Vestergaard, E. Lægsgaard, I. Stengsgaard, F. Besenbacher, Science 303 (2004) 511.
[26] L.M. Molina, B. Hammer, Phys. Rev. Lett. 90 (2003) 206102.
[27] I.N. Remediakis, N. Lopez, J.K. Nørskov, Angew. Chem. Int. Ed. 44 (2005) 1824.
[28] E. Wahlström, N. Lopez, R. Schaub, P. Thostrup, A. Rønnau, C. Africh, E. Lægsgaard, J.K. Nørskov, F. Besenbacher, Phys. Rev. Lett. 90 (2003) 026101.
[29] The DACAPO plane wave/pseudopotential DFT code is available as Open Source Software at http://www.fysik.dtu.dk/CAMPOS/.
[30] D. Vanderbilt, Phys. Rev. B 41 (1990) 7892.
[31] B. Hammer, L.B. Hansen, J.K. Nørskov, Phys. Rev. B 59 (1998) 7413.
[32] M.C. Payne, M.P. Teter, D.C. Allan, T.A. Arias, J.D. Joannopou-los, Rev. Mod. Phys. 64 (1992) 1045.
[33] G. Kresse, J. Furthmüller, Comput. Mater. Sci. 6 (1996) 15.
[34] M.D. Rasmussen, L.M. Molina, B. Hammer, J. Chem. Phys. 120 (2004) 988.
[35] A. Eichler, J. Hafner, Phys. Rev. B 59 (1999) 5960.
[36] N. Lopez, J.K. Nørskov, Surf. Sci. 515 (2002) 175.
[37] R. Schaub, P. Thostrup, N. Lopez, E. Lægsgaard, I. Stensgaard, J.K. Nørskov, F. Besenbacher, Phys. Rev. Lett. 87 (2001) 266104.
[38] D.C. Meier, D.W. Goodman, J. Am. Chem. Soc. 126 (2004) 1892.
[39] M. Valden, S. Pak, X. Lai, D.W. Goodman, Catal. Lett. 56 (1998) 7.

[40] G.R. Bamwenda, S. Tsubota, T. Nakamura, M. Haruta, Catal. Lett. 44 (1997) 83.
[41] T.V. Choudary, C. Sivadinarayana, C.C. Chusuei, A.K. Darye, J.P. Fackler, D.W. Goodman, J. Catal. 207 (2002) 247.
[42] B. Schumacher, Y. Denkwitz, V. Plzak, M. Kinne, R.J. Behm, J. Catal. 224 (2004) 449.
[43] S. Kandoi, A.A. Gokhale, L.C. Grabow, J.A. Dumesic, M. Mavrikakis, Catal. Lett. 93 (2004) 93.
[44] S.A. Varganov, R.M. Olson, M.S. Gordon, G. Mills, H. Metiu, J. Chem. Phys. 120 (2004) 5169.
[45] I. Chorkendorff, J.W. Niemantsverdriet, Concepts of Modern Catalysis and Kinetics, Wiley–VCH, 2003.
[46] M.S. Chen, D.W. Goodman, Science 306 (2004) 252.
[47] Y. Morikawa, private communication.
[48] T. Hayashi, K. Tanaka, M. Haruta, J. Catal. 178 (1998) 566.